XX IMEKO World Congress
Metrology for Green Growth
September 9–14, 2012, Busan, Republic of Korea

EXPERIMENTAL INVESTIGATION ON RADIATED EMISSIONS GENERATED BY PANTOGRAPH ARCING AND THEIR EFFECTS ON TELECOMMUNICATION BANDS

A. Mariscotti[1], A. Marrese[2], N. Pasquino[2]

[1]Dept. of Naval and Electrical Engineering, University of Genoa, Via all'Opera Pia 11/A, Genoa, Italy
[2]Dept. of Electrical Engineering, University of Naples Federico II, Via Claudio 21, Naples Italy

Abstract: The paper investigates the radiated emissions caused by the interaction between pantograph and overhead lines in electrical transportation systems, and their effects on the frequency band occupied by some used telecommunication systems. Transient amplitude, rise time and pulse duration are measured in time domain to obtain the associated empirical distributions; power spectrum and frequency content are calculated in the bands of interest; finally a time-frequency representation is used to track the evolution of spectral components over time.

Keywords: electromagnetic compatibility; time-domain measurements; radiated disturbances; pantograph arcing.

1. INTRODUCTION

The infrastructure of an electrified transportation system is a complex system that consists of electrical substations (power generation), overhead contact wires and rails (power transmission), switches and trains (loads), and the signaling system. The system is characterized by electromagnetic phenomena spanning over a very large frequency interval: thyristor chopper, used in DC-fed trains, can generate electromagnetic disturbance up to 400 Hz, possibly extending to a few kHz in the presence of more than one chopper circuit [1], which produces a wide spectrum of harmonics [2]; traction drives with IGBT transistors can produce interferences at frequencies of some MHz [3], while *corona* effect may produce electromagnetic interferences even above tens of MHz [4]. Furthermore, switching operation in electrical substations can generate disturbances up to the VHF band [5].

Electromagnetic compatibility standards such as the EN 50121 series [6] characterize emission and immunity of the transportation system and its components (rolling stock and signaling systems) without specific focus on the interaction between the pantograph and the contact wire because its transient nature makes it less a significant threat to the functional features of electronic systems and in turn to safety requirements. Nonetheless, such interaction is a primary cause of interferences because the arcing ignited in the air gap between the pantograph and the overhead wire causes distortion of voltage and current waveforms in the power system.

Due to mechanical oscillations, rapid detaching of the pantograph from the wire can occur followed by reattaching after a short time. This triggers an electric arc which generates wideband noise possibly covering frequencies up to a few GHz [7]. Detachments can be facilitated by the use of several pantographs on the same train, by the presence of more than one overhead cable [8], or by the existence of such structures in the overhead line like switches and section breakers. Moreover, small arcs can be produced by sliding contact due to micro-irregularities, oxide or dust between the two surfaces [9].

Arcing is seen as one of the most significant phenomena that concur in the determination of the electromagnetic compatibility features of the whole transportation system at high frequencies, with electric and electromagnetic characteristics depending on many parameters like voltage, weather conditions, electrical contacts [9]-[10].

Our interest for the pantograph/catenary sub-system is due to the possible effect on telecommunication systems, such as GSM, UMTS and Wi-Fi due to the large spectra characterizing the radiated disturbance produced by the arc. Most of the experiments described in the previously mentioned research papers were run in a controlled environment, like a lab where a pantograph/contact line mock-up was build so that the parameters affecting the arc characteristics were controllable and fixed at known levels. Continuing and extending the study in [11], authors have carried out experiments in a real environment by measuring the radiated disturbance on board a DC-powered train during a regular journey, so to determine the actual disturbances encountered by devices operating in one of the bands of interest during normal use.

2. MEASUREMENT SETUP

Measurements were carried out on a 1500 V DC electrified transportation system run by Circumvesuviana s.r.l., an Italian local transportation service, whose network extends over 140 km with 6 lines and 96 passengers stations. The maximum speed is 90 km/h and a typical speed profile is shown in Fig. 1: acceleration at departure from one station is followed by one or more coasting/acceleration stages until braking is activated close to the arrival station. The average speed is around 60 km/h, while the commercial speed

(average speed including station stops) is 38 km/h. The measurement campaign was run on a return trip between Naples and Sorrento (Italy) for a total of 86 km on a Metrostar ETR200 train, built by AnsaldoBreda-Firema.

The measurement system is a tripod-mounted HE300 array-log antenna by Rohde & Schwarz sensing the electric field in the range from 0,5 to 7,5 GHz, connected through a coaxial cable to an SDA6000A digital oscilloscope with 6 GHz analog bandwidth and 20 GS/s sampling frequency.

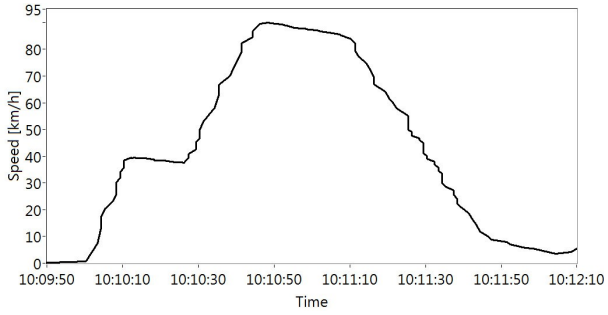

Figure 1. Typical speed profile between two stations with accelerations, coasting and braking.

The antenna (Fig. 2) is placed on the coach's floor at about 2.5 m from the pantograph's projection. It is vertically polarized and tilted so to point at the pantograph and maximize the received disturbance level.

Figure 2. Measurement setup shown from outside and inside the train.

Due to the transient nature of the disturbances, signals have been measured in the time domain and post-processed for frequency and time-frequency analysis. Moreover, the ambient noise makes the setup of the oscilloscope quite critical. In fact, in some cases the pulse amplitude is comparable to the noise's one. Therefore the trigger level of the oscilloscope has been set adaptively, based on a compromise between sensitivity to low-amplitude transients and rejection of background noise generated by near-by sources transmitting in the same band.

The DSO was set to acquire 10 successive triggers of 100 kSa points each (covering a 5 μs time interval each) and then send the whole batch of acquired windows to a laptop through a TPC/IP cable (for faster connection).

Pulse amplitude, rise time and duration have been obtained and the experimental distributions compared to some theoretical *pdf*'s; in the frequency domain the average power spectrum has been calculated to determine the frequency range containing most of the radiated noise power; in the joint time-frequency domain, the power spectrum's evolution over time has been observed, to highlight the time interval during which the disturbances are more critical.

3. RESULTS

Fig. 3 shows the histogram of absolute frequency of transient events per kilometer versus train speed. It can be seen that most events occur around 30 km/h, i.e. at the speed kept when the train approaches overhead and rail switches where typically a lot of interruptions in the pantograph/overhead wire contact occur, with consequent generation of arcs.

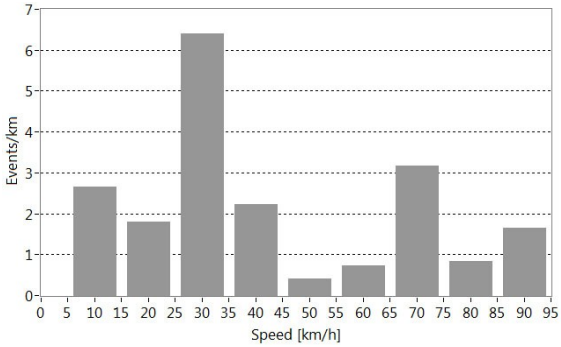

Figure 3. Transient events per kilometer versus train speed.

A. Time-domain analysis

Fig. 4 shows a typical transient profile over time with the indications of the pulse amplitude *A*, rise time *RT* (time to rise from 10% to 90% of the peak of the absolute value) and pulse duration *D* (time during which the pulse is above 50% of the peak of the absolute value).

Fig. 5 shows the amplitude *A* in dB arbitrary units versus speed. The correlation coefficient is about 0.6, thus speed does not seem to be a relevant factor. The events measured at zero speed were not included, as they refer to a steady condition in which arcing is ignited by oscillations of the overhead wire due to wind of other trains. Moreover, pulse amplitudes above -20 dB observed at about 30 km/h have been considered as outliers by the regression algorithm and therefore excluded from the calculation of the correlation coefficient. It must be noted that the acquired samples have not been filtered to reject the background noise that in some cases may have altered the measured amplitude, for instance when the disturbance is superimposed to a strong video broadcast, GSM or UMTS signal.

The experimental distributions of the amplitude, rise time and duration were compared to some reference distributions (Fig. 6) with parameters estimated with a

maximum likelihood approach. Amplitude distribution is better described by a Log-logistic (matching findings in [11], while the differences with the GEV distribution mentioned in [12] are minimal), the rise time by an Exponential and the pulse duration by a Weibull.

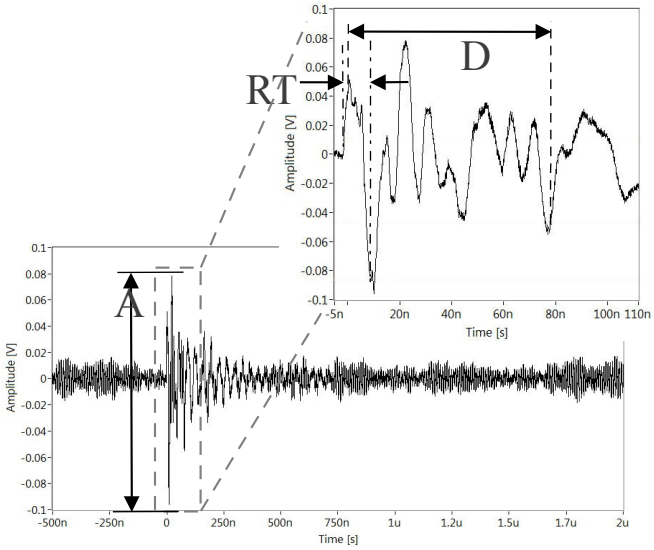

Figure 4. Transient time profile: A is the amplitude, D is the time duration, RT is the rise time.

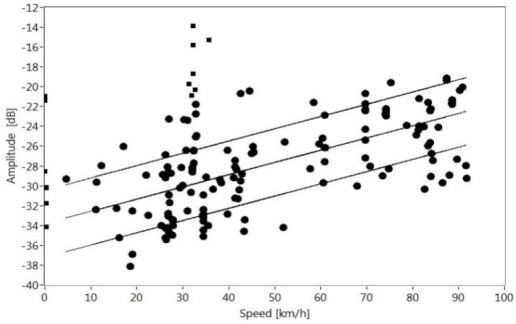

Figure 5. Transient amplitude versus train speed.

B. Frequency-domain analysis

To compare the spectral content of the pulse to that of the other signals existing at the same time, an FFT computed from samples acquired over 500 ns *before* the transient has been compared to the FFT from samples acquired *during* the transient over the same time length. The average of 69 different events gives the two spectra shown in Fig. 7, which shows that the frequency content is mainly located in the low frequency end, where the pulse is 10 to 15 dB higher than the background noise, and that the difference decreases to less that 5 dB from 1.7 GHz onward.

C. Time/frequency-domain analysis

Given the transient nature of the phenomena under observation, a pure frequency-domain analysis would lack time resolution. Therefore, a joint time-frequency analysis has been carried out to determine the time behaviour of the pulse spectral content within the bands of some telecommunication systems like GSM, GSM-R, DCS, UMTS and WiFi.

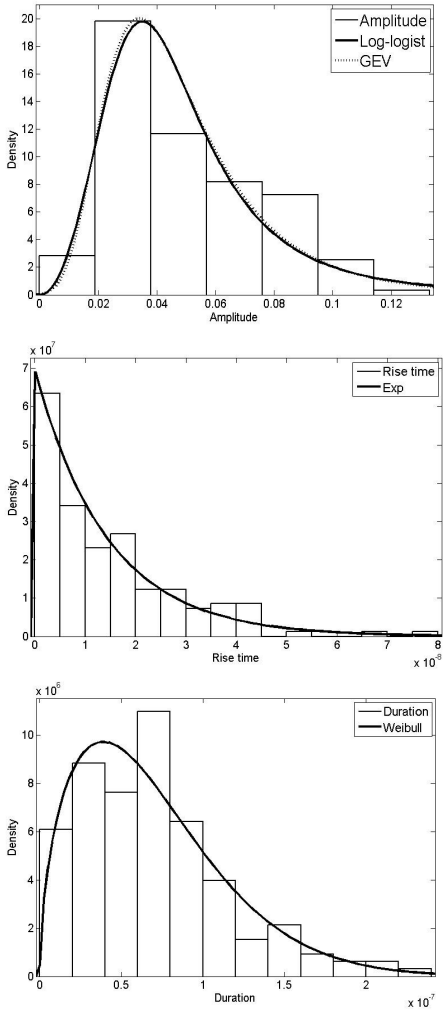

Figure 6. Experimental pdf's of: a) transient's amplitude; b) rise time; c) duration

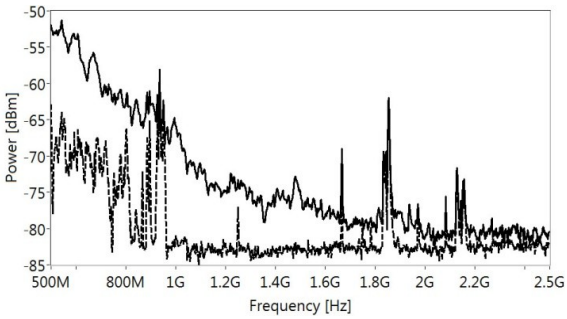

Figure 7. Average of 69 FFT's calculated over a 500 ns time window: interval before (dashed) and during (solid) the transient event.

An appropriate time/frequency representation is to be chosen, because of the trade-off between the time- and frequency-resolution features and the unavoidable presence of interference terms [13]. We focused on two different representations, namely the *Short Time Fourier Transform* (STFT) and the *Smoothed Pseudo Wigner-Ville* (SPWV) distribution, whose details can be found in [13]. These two representations provide a fairly good interference rejection, yet limiting the localization capabilities. We preferred them over a higher-resolution Choi-Williams kernel, because the

latter presents large cross-terms interfering with the detection of the auto-terms present in the same ranges.

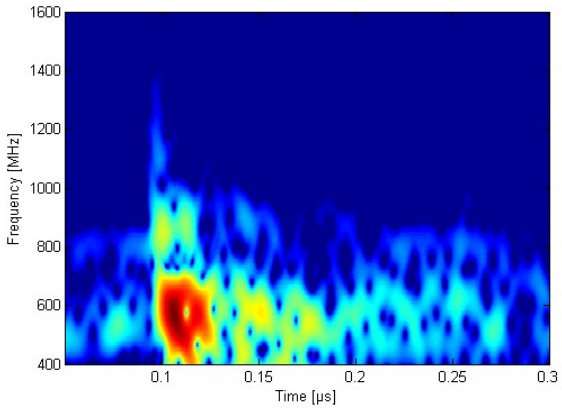

Figure 8. STFT calculated with a 160-point Hanning window.

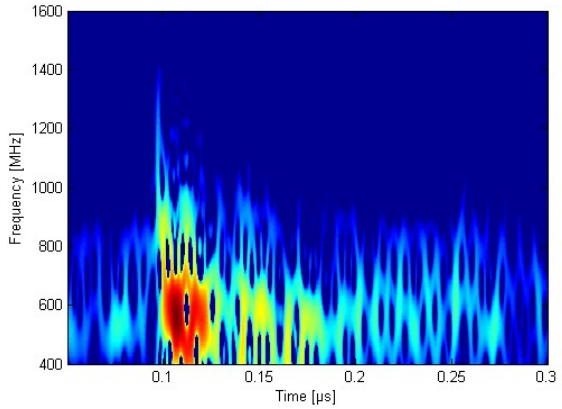

Figure 9. SPWV calculated with a 40-point and 80-point Hanning window for the time and frequency axis respectively.

Fig. 8 shows the STFT of a typical pulse, calculated with a time-window length of 8 ns (a 160-point Hanning window with a 50 ps sampling time) and a 4096-point FFT (obtained from the 8 ns window with zero-padding), resulting in a fictitious 4.88 MHz resolution. These values have been determined empirically as those with the best balance between time and frequency resolution. The arc-generated pulse is clearly visible in the spectrogram as the area with lighter colors. The power content associated with the transient is superimposed to that of some telecommunication systems whose footprint is visible in the low end, from 500 to 800 MHz and above. Most of the radiated power's frequency content spans over the range from 500 MHz (the antenna's lower bound) up to 1 GHz, a band largely occupied by the Italian TV broadcasting service. Some additional contributions are present up to 1.4 GHz although their limited time extension makes them not significant. The power peak persists for about 25 ns while after 100 ns its level becomes comparable with the background emissions. Fig. 9 shows the SPWV representation for the same signal, obtained with the most appropriate time and frequency resolution parameters (time smoothing window length of 2 ns, frequency smoothed window length of 4 ns and 2048 frequency bin resulting in a fictitious 4.88 MHz resolution) to reject the cross (i.e. interference) terms. It can be noted that the picture shows a slightly better time resolution as opposed to an equivalently slightly worse frequency resolution. It is noticeable that the time-frequency behaviours shown in both figures point out that telecommunication systems are affected differently over time.

4. CONCLUSIONS

The time-, frequency- and joint time-frequency domain characteristics of the radiated disturbances generated by the interaction between the pantograph and overhead wire have been reported. Experiments show that the impulsive nature of the phenomena spread the spectral content over a wide frequency band, possibly affecting telecommunication systems. However, the pulse typical time duration makes the phenomenon not a relevant threat to telecommunication QoS unless their repetition frequency is high enough to affect a significant number of bits.

5. REFERENCES

[1] R. J. Hill, “Electric railway traction. VI. Electromagnetic compatibility disturbance-sources and equipment susceptibility,” Power Engineering Journal, vol 11, issue 1, pp. 31-39, February 1997

[2] Z.A. Styczynski, S. Bacha, A. Bachry and L. Etxeberria, “Improvement of EMC in railway power networks,” Harmonics and Quality of Power, 2002. 10th International Conference on, vol. 2, pp. 754-759, Oct. 2002

[3] G. Busatto, L. Fratelli, C. Abbate, R. Manzo and F. Iannuzzo, “Analysis and optimisation through innovative driving strategy of high power IGBT performances/EMI reduction trade-off for converter systems in railway applications" Microelectronics Reliability, vol. 44, pp. 1443-1448, 2004

[4] S. K. Nayak and M. J. Thomas, “Computation of EMI fields generated due to corona on high voltage over head power transmission lines,” Proceedings of the International Conference on Electromagnetic Interference and Compatibility. 2002.

[5] E. J. Bartlett, M. Vaughan and P. J. Moore, “Investigations into electromagnetic emissions from power system arcs,” International Conference and Exhibition on Electromagnetic Compatibility. 1999.

[6] EN 50121, “Railway applications - Electromagnetic compatibility”

[7] S. Leva, A. P. Morando and R. E. Zich, “On the unwanted Radiated Fields due to Sliding Contacts in a Traction System,” IEICE Transactions on Communications. Mar 2000, Vol. E83-BNO.3, p. 519-524.

[8] S Brillante, P. Ferrari and P. Pozzobon, “Modelling of electromagnetic emission from catenary-pantograph sliding contact,” Transactions on the Built Environment. 1998, Vol. 34

[9] S. Midya, D. Bormann, A. Larsson, T. Schutte, and R. Thottappillil, "Understanding pantograph arcing in eletrified railways – Influence of various parameters," *Proc. IEEE Symp. Electromagnetic Compatibility*, Detroit, MI, Aug. 2008, pp 1-6

[10] S. Midya, D. Bormann, A. Larsson, T. Schutte, and R. Thottappillil, "Pantograph Arcing in Electrified Railways—Mechanism and Influence of Various Parameters—Part I: With AC Traction Power Supply," *IEEE Trans. Power Delivery*, vol. 24, no. 4, Oct. 2009, pp. 1940-1950

[11] A. Mariscotti and V. Deniau, “On the characterization of pantograph arc transient on GSM-R antenna,” 17th Symposium IMEKO TC 4, 3rd Symposium IMEKO TC 19 and 15th IWADC Workshop. 2010.

[12] N. Ben Slimen, V. Deniau, J. Rioult, S. Dudoyer and S. Baranowski, “Statistical Characterisation of the EM Interferences Acting on GSM-R Antennas Fixed Above Moving Trains,” *The European Physical Journal – Applied Physics*. 2009, Vol. 48, 21202

[13] F. Hlawatsch and F. Auger, *Time-Frequency Analysis*, October 2008, Wiley-ISTE, ISBN: 978-1-84821-033-2